Coordination Chemistry Reviews 253 (2009) 2306–2314

Contents lists available at ScienceDirect

Coordination Chemistry Reviews

journal homepage: www.elsevier.com/locate/ccr

Review

Cyanometalate-bridged oligonuclear transition metal complexes—Possibilities for a rational design of SMMs

Mihail Atanasov[a,b], Peter Comba[a,*], Sascha Hausberg[a], Bodo Martin[a]

[a] Universität Heidelberg, Anorganisch-Chemisches Institut, Im Neuenheimer Feld 270, 69120 Heidelberg, Germany
[b] Institute of General and Inorganic Chemistry, Bulgarian Academy of Sciences, Acad. Georgi Bontchev Str. Bl.11, 1113 Sofia, Bulgaria

Contents

ARTICLE INFO

Article history:
Received 4 December 2008
Accepted 26 January 2009
Available online 11 February 2009

Keywords:
Molecular magnetism
Single-molecule magnet (SMM)
Magnetic exchange
Magnetic anisotropy
Hexacyanometalate
Ligand field theory
DFT

ABSTRACT

The anisotropy barrier and blocking temperature of single-molecule magnets (SMMs) depend on the total spin S (and therefore to some extent on the size of the molecule) as well as on the Ising-type axial magnetic anisotropy D. There is a relatively large anisotropy of the magnetic exchange across cyanide bridges and therefore, moderate-sized oligonuclear complexes may lead to appreciably high anisotropy barriers. Also, the geometry of cyanide bridges and the preference of metal ions for a specific linkage isomer allow predicting oligonuclear structures based on relatively simple building blocks of low nuclearity. Theoretical approaches have been developed to understand the nature of the magnetic exchange through the cyanide bridge and to predict magnetic exchange and anisotropy of larger spin clusters on the basis of theoretical approaches which combine ligand field theory with DFT-based methods. These models and consequences for the design and synthesis of SMM materials are discussed in detail.

1. Introduction

$[Mn_{12}O_{12}(OOCCH_3)_{16}(OH_2)_4]$ (Mn_{12}, see Fig. 1), was first prepared and characterized in 1980 [1] and discovered in the early 1990s to exhibit magnetic bistability [2–5]. Its $Mn^{III}O_6$ octahedra are elongated due to Jahn–Teller coupling, and this leads to a negative axial zero-field splitting D and, consequently, to removal of the degeneracy of the M_S sublevels of the $S = 10$ ground state, such that those with the largest M_S values are the lowest in energy (see Fig. 2). The thermal energy for interconversion of the two $M_S = \pm 10$ states is $U = S^2|D|$ for integer values of S, such as for Mn_{12} with $M_S = +10$ and $M_S = -10$, and $U = (S^2 - (1/4))|D|$ for half-integer values of S. The experimentally determined barrier U_{eff} for Mn_{12} is approximately 50 cm^{-1}, and this agrees with the expectation derived from $S = 10$ and $D = -0.5$ cm^{-1} and results in a blocking temperature of $T_B = 3.8$ K and a relaxation time τ of about 2 months at 2 K [6,7]. Molecules like Mn_{12} behave like classical magnets at very low temperature and are called single-molecule magnets (SMMs) [8]. The bistability of SMMs together with their size of 2–5 nm may open the way to magnetic information storage materials of unprecedented density. In addition, SMMs are of interest in fundamental science as unique examples to study quantum effects, and they have also attracted attention in the fields of quantum computing, magnetic refrigeration and spin-based molecular electronics [9,10].

The field has seen much activity in the last decade and much of the physics and theoretical basis of SMM properties as well as interesting experimental approaches for the characterization of novel magnetic materials have been developed. However, while a number

* Corresponding author at: Universität Heidelberg, Anorganisch-Chemisches Institut, Im Neuenheimer Feld 270, 69120 Heidelberg, Germany.
Fax: +49 6221 546617.
E-mail address: peter.comba@aci.uni-heidelberg.de (P. Comba).

0010-8545/$ – see front matter © 2009 Elsevier B.V. All rights reserved.
doi:10.1016/j.ccr.2009.01.033

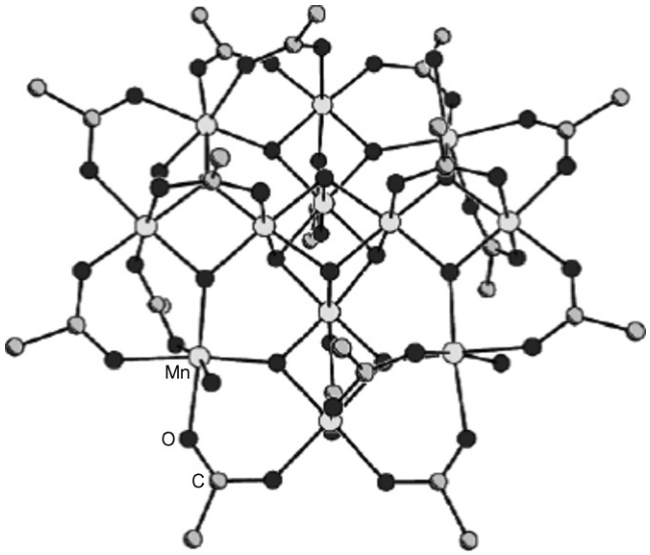

Fig. 1. Experimental structure of Mn_{12} (light gray: Mn, black: oxygen, dark gray: carbon) [1] (reproduced from [101]).

of new SMMs have been prepared and thoroughly characterized, so far there is only one example with a slightly larger anisotropy barrier and blocking temperature than Mn_{12} ($U_{eff} = 86.4\,cm^{-1}$, $T_B = 4.5$ K) [11]. One reason for the slow progress in the synthesis of SMMs is that, while the most crucial parameters for a significant increase of the anisotropy barrier are known – a large and negative value of the axial zero field splitting and a large total spin – a more than qualitative prediction of D has rarely been achieved, in contrast, to some extent at least, to the prediction of S, based on well understood magnetic coupling mechanisms [12]. Lower than expected values or the wrong sign of D are major problems in a successful development of SMMs [13,14], and phonon-assisted loss, quantum tunneling of the magnetization, as well as transversal anisotropies due to off-axial geometries are other problems which limit the increase of the blocking temperature [9].

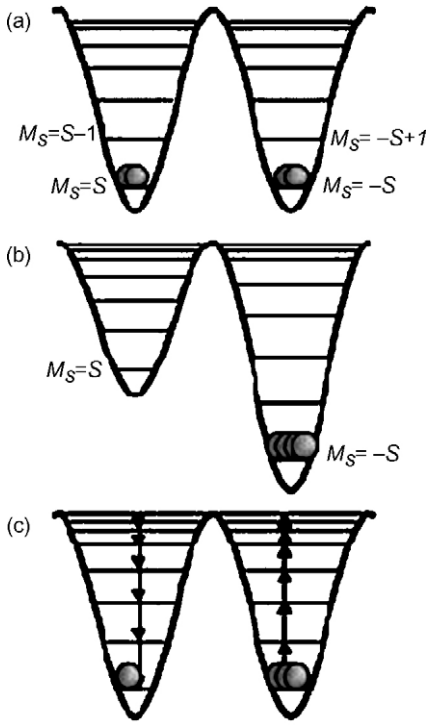

Fig. 2. Energy levels for a spin state S with an easy axis magnetic anisotropy as in Mn_{12} (see Fig. 1). (a) Energy levels and population at zero magnetic field: the +M and −M levels are equally populated. (b) A magnetic field lifts the degeneracy of the +M and −M levels and selectively populates the −M levels. (c) After removal of the magnetic field the system is equilibrated; the rate of equilibration depends on the energy barrier U between the two M_s ground states (reproduced from [9]).

With a combined ligand-field-theory and broken-symmetry DFT approach (LFDFT) we have been able to show that the ground state Jahn–Teller coupling has strong implications for the isotropic and anisotropic magnetic exchange in oligonuclear cyanometalate complexes [13]. The LFDFT model was used for the qualitative discussion of the magnetic properties of published oligonuclear transition metal complexes with ferromagnetic ground states [13] and for a thorough analysis of a series of linear and bent trinuclear hexacyanoferrate-based complexes [14]. The absence of SMM behavior in the latter examples was due to large angular distortions of the $[Fe(CN)_6]^{3-}$ sites, imposed by electronic, ligand-based steric and/or crystal lattice effects and concomitant quenching of orbital angular momentum of the Fe^{III} ($^2T_{2g}$) ground state.

While qualitative rules emerge from the LFDFT model [13,14], so far unpredictable subtle distortions lead to magnetic anisotropies which generally are smaller than expected and required for SMM behavior. It immediately follows that a reliable structure prediction is needed for an efficient design of novel cyanometalate-based SMMs, and it appears that only MM-based approaches will be able to efficiently and reliably lead to the desired results [15]. Due to the importance of Jahn–Teller-labile centers such as $[Fe(CN)_6]^{3-}$, the LFMM approach [16–20] appears to be the method of choice although this has not yet been tested for oligonuclear cyanometalates. Two additional challenges are that the modeling of complexes with simple monodentate ligands is particularly difficult (no forces exerted by the ligand backbone) [15], and that from the experimental studies so far, it appears, not unexpectedly, that crystal lattice effects might be of importance. The optimization of crystal lattices is somewhat more difficult but the basic principles follow the same rules as those of MM of isolated molecules, and corresponding approaches have been developed [21–23] and methods for the crystal structure prediction have also been described [24–26].

2. Magnetic exchange through the cyanide bridge

Theoretical work on the magnetic exchange via CN^--bridged transition metal centers has been carried out on dinuclear model complexes, and various approaches, including a valence bond configuration interaction model [27,28], methods based on Extended Hückel calculations [29,30], the Kahn–Briat exchange coupling model [31,32], the augmented spherical waves model [33], Hartree-Fock [34,35] and DFT calculations [35–38] have been used. An efficient coupling mechanism via CN^- π-orbitals, in particular for t_{2g}^4–t_{2g}^3 ($Mn^{III}V^{II}$), t_{2g}^3–t_{2g}^3 ($Mo^{III}V^{II}$), t_{2g}^3–t_{2g}^4 ($Cr^{III}Mo^{II}$), t_{2g}^2–t_{2g}^3 ($V^{III}V^{II}$) and t_{2g}^3–t_{2g}^3 ($Cr^{III}V^{II}$) metal pairs, gives rise to strong antiferromagnetic coupling. The combination of π donation (for M^{III}) and π back-donation (for M^{II}) is of importance, and ferromagnetic coupling was found in the t_{2g}^3–$t_{2g}^6e_g^2$ $Mn^{IV}Ni^{II}$ pair [37]. With a broken-symmetry DFT approach the exchange coupling constant was related to σ-, π- and π*-type spin densities of the CN^- bridge (see Fig. 3) [38]. In Cu^{II}–M^{III} pairs the $^2B_{1g}$ (d_{x2-y2}) ground state of Cu^{II} leads to ferromagnetic exchange, dominated by π delocalization via the CN^- π pathway. Spin polarization, due to overlap of the doubly occupied σ orbitals of CN with the empty d_{z2} orbital of M^{III} and π* orbitals of CN^-, yields negative spin occupations in these orbitals and reduces the Cu^{II}–M^{III} exchange coupling. When the d_{z2} orbital of M^{III} is singly occupied, an additional positive spin density appears in the σ(CN) orbital and leads to an increase of the ferromagnetic Cu–NC–M exchange constant [38]. For Cu^{II} in a $^2A_{1g}$

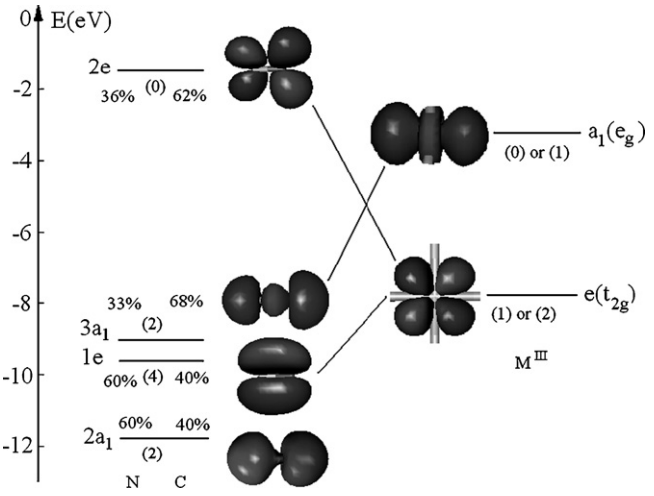

Fig. 3. Orbitals of the CN^- bridges coupled with the e_g and t_{2g} orbitals of the transition metal ion M^{III} (reproduced from [38]).

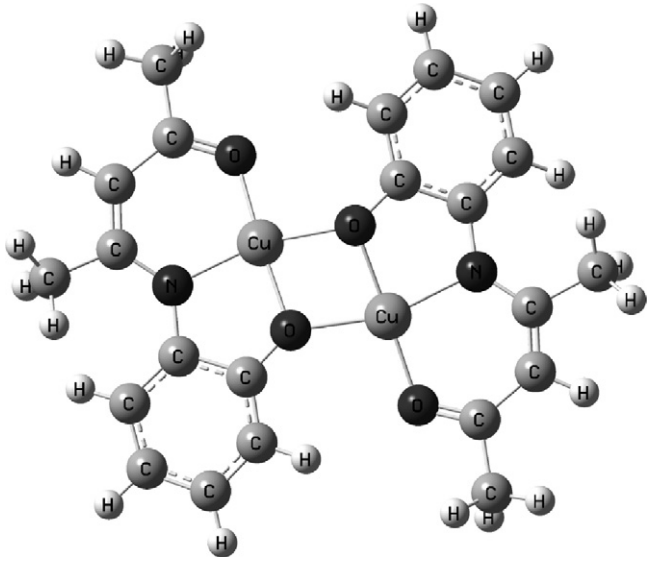

Fig. 4. Plot of the experimental structure of the bisphenolate-bridged dicopper(II) complex with $J_{exp} = -298\ cm^{-1}$, used for the benchmark broken-symmetry DFT computation of the exchange coupling (see Table 1) [41,42].

(d_{z2}) ground state, with the tetragonal axis parallel to the Cu–NC–Fe bridge, spin polarization leads to σ-type β spin-densities on CN and an antiferromagnetic Cu^{2+}–CN–radical coupling, and therefore induces an exchange pathway which enhances the ferromagnetic Cu–Fe exchange coupling [13].

Exchange coupling between transition metal ions with non-degenerate ground states (e.g., Ni^{II}–NC–Cr^{III}) can be calculated with acceptable accuracy (see Section 3). However, with Kohn–Sham DFT it generally is not possible to thoroughly account for orbital degeneracy [39,40]. Therefore, a novel approach has been developed to treat Jahn–Teller coupling with ions such as Mn^{III} and Fe^{III} in their low-spin orbitally degenerate ground states ($^3T_1$ and $^2T_2$) [40]. Jahn–Teller distortions are weak for the π ground states of Mn^{III} (t_{2g}^4) and Fe^{III} (t_{2g}^5). DFT values of the exchange coupling parameters from different occupations of the t_{2g} orbitals of low-spin (t_{2g}^5) Fe^{III} as well as spin-orbit coupling have been used to characterize the isotropic and anisotropic exchange coupling constant in the linear Cu–NC–Fe exchange pair [38]. It is important to be cautious when calculating exchange coupling constants with the broken-symmetry DFT method, especially with transition metal ions with T_1 and T_2 orbitally degenerate states, because mixing between various configurations via spin-orbit coupling can strongly modify the DFT-predicted values of the exchange coupling constants (see also Section 3).

General conclusions from our studies [38,40] on the magnetic coupling across the CN^- bridge are that (i) it is governed by pathways which involve π [$t_{2g}(d_{xz,yz})$, 1e(CN)], π*[$t_{2g}(d_{xz,yz})$, 2e(CN)], as well as σ [$e_g(d_{z2})$, $3a_1$(CN)] M–CN-based orbitals. (ii) If the d_{z2} orbital is empty, CN → M transfer leads to β spin density on the C and N atoms of the CN bridge, and this decreases the magnitude of the Cu–M exchange coupling, which is dominated by α spin densities. If the d_{z2} orbital is singly occupied, both σ and π spin densities are of α type, and this enhances the ferromagnetic exchange interaction. For the strong CN^- bridging group, the d_{z2} orbital is singly occupied in the high-spin configuration, and this leads to metastable excited states. (iii) A novel approach to calculate magnetic exchange coupling constants, based on the calculation of spin densities of dinuclear Cu^{II}–NC–M^{III} building blocks has been developed; this involves the calculation of the spin density on the CN^- bridge of the M^{III}–CN fragment, followed by the computation of the coupling of a CN radical with the Cu^{II} complex. Because DFT generally overestimates metal-ligand covalency, the emerging values of J are systematically larger than those from broken-symmetry calculations. However, the new approach allows one to analyze the exchange coupling across the CN^- bridge in terms of the various pathways, i.e. involving the σ, π and π* orbitals of CN^-, and the application to the Cu^{II}–CN–M^{III} pairs shows that ferromagnetic exchange is dominated by spin delocalization over the fully occupied CN^- π orbital. (iv) Jahn–Teller coupling is small in the $^3T_{1g}$ state of $[Mn(CN)_6]^{3-}$ (t_{2g}^4) and very small for the $^2T_{2g}$ state of $[Fe(CN)_6]^{3-}$ (t_{2g}^5). The resulting stabilization of the non-degenerate $^3A_2$ and $^2B_2$ ground states leads to a weak ferromagnetic coupling in the case of the Cu^{II}–Mn^{III} pair, and a very small isotropic exchange coupling parameter for the Cu^{II}–Fe^{III} pair. (v) The orbital dependence of the exchange coupling leads to a large anisotropy in linear Cu^{II}–NC–Fe^{III} pairs and to an even larger anisotropy in Cu^{II}–Fe^{III}–Cu^{II} and Mn^{II}–Fe^{III}–Mn^{II} trinuclear complexes [14].

3. Coupling constants computed by broken-symmetry DFT

In order to validate the more conventional DFT-based approach for calculating exchange coupling constants of oligonuclear transition metal complexes, the bisphenolate-bridged dicopper(II) complex shown in Fig. 4 ($J_{exp} = -298\ cm^{-1}$ [41,42]) has been used to optimize the method for a broken-symmetry-DFT-based computation of exchange coupling constants (see Table 1), and the method has then been validated with a large series of experimentally known oligonuclear complexes [43]. The computations are based on a

Table 1
Exchange coupling constant J of the dicopper(II) complex shown in Fig. 4, calculated with different functionals and basis sets, using Eq. (1) [43].

Method	CPU time [h][b]	J_{calc} [cm^{-1}] ($J_{exp} = -298\ cm^{-1}$ [41,42])
B3LYP/TZV	4.60	−231.11
B3P86/TZV	3.71	−241.04
B3PW91/TZV	3.44	−227.46
BLYP/TZV	4.00	−854.24
BP86/TZV	4.26	−879.53
BPW91/TZV	4.20	−848.04
PBE/TZV	4.31	−853.74
SVWN/TZV	5.07	−1181.13
B3LYP/3-21G	0.56	−113.95
B3LYP/TZVP	4.60	−231.11
B3LYP/6-31G*_TZVP[a]	2.38	−239.32

[a] TZVP for Cu^{II} and the donor atoms, 6-31G* for the remaining atoms.
[b] QuadCore Q9450 (one processor), 8GB RAM.

Table 2
Comparison of calculated and experimental J values of a series of oligonuclear complexes (J_{calc} and J_{opt} are obtained with Eq. (1), J_{calc} is derived from the experimental structure (calculated with Jaguar, B3LYP/6-31G*_LACV3P++**) and J_{opt} from the DFT-refined structure (high-spin state, calculated with Orca, B3LYP/6-31G*_TZVP); see original publication for structures of the complexes) [43].

Compound	J_{calc} [cm^{-1}]	J_{opt} [cm^{-1}]	J_{exp} [cm^{-1}]	References
$[Cu_2(MeC(OH)(PO_3)_2)_2]^{4-}$	−103.0	−118.2	−30.9	[121,122]
$[(Et_5dien)_2Cu_2(\mu\text{-}C_2O_4)]^{2+}$	−99.0	−112.2	−37.4	[122,123]
$[Mn(NH_3)_4Cu(oxpn)]^{2+}$	−40.8	−37.0	−15.7	[122,124]
$[(\mu\text{-}OCH_3)VO(maltolato)]_2$	−84.3	−83.4	−107.0	[122,125]
$[Fe_2OCl_6]^{2-}$	−148.0	−109.5	−112.0	[122,126]
$[MnMn(\mu\text{-}O)_2(\mu\text{-}OAc)DTNE]^{2+}$	−156.3	−117.9	−110.0	[122,127]
$[Cu_2(\mu\text{-}OH)_2(bipym)_2]^{2+}$	95.8	−98.5	57.0	[122,128]
$[(Dopn)Cu(OH_2)Cr(OCH_3)L]^{2+}$	12.8	31.5	18.5	[122,129]
$[(Dopn)Cu(\mu\text{-}CH_3COO)MnL]^{2+}$	54.2	54.9	54.4	[122,129]
$[V_2O_2(\mu\text{-}OH)_2([9]aneN_3)_2]^{2+}$	−241.8	−52.5	−177.0	[130,131]
$[Et_3NH]_2[(VO)_2(BBAC)_2]$	−160.9	−81.6	−167.9	[131,132]
$[HB(pz)_3VO(OH)_2]_2$	14.3	29.2	−38.8	[131,133]
$[(VO)_2(cit)(Hcit)]^{3-}$	−267.8	−29.0	−212.0	[131,134]
$[V_2O_2(\mu\text{-}OH)(tpen)]^{2+}$	−461.7	−19.1	−150.0	[131,135]
$[(VO)_2L(\mu\text{-}SO_4)]$	−132.6	−121.9	−128.0	[131,136]
$[V_2O_2(OH)(C_4O_4)_2(H_2O)_3]^{-}$	−245.7	−211.2	−117.0	[131,137]
$[(VO)(3\text{-hydroxy-3-methylglutarate})]_2^{2-}$	8.9	−2.5	1.5	[131,138]
$[(VO(Hsabhea))(VO(acac)(HOMe))(\mu_2\text{-}OMe)]$	18.6	15.4	5.3	[131,138]
$[Cu_2(tren)_2CN](ClO_4)_3$	−98.6	−98.3	−79.0	[139]
$[Cu_2(tren)_2CN](BF_4)_3$	−119.1	−71.9	−80.0	[139]
$[Cu_2(tren)_2CN](ClO_4)(PF_6)_2$	−77.0	−79.2	−91.5	[139]
$[Cu_2(tmpa)_2CN](ClO_4)_3$	−70.1	−57.8	−52.0	[139]
$[Cu_2(tmpa)_2CN](BF_4)_3$	−69.8	−57.9	−50.0	[139]
$[Cu_2(tmpa)_2CN](BF_4)_3{\cdot}(CH_3CN)_2$	−76.9	−57.9	−49.5	[139]
$[Ni_2(tetren)_2CN][Cr(CN)_6]$	−15.4	−9.3	−12.5	[139]

Heisenberg–Dirac–van Vleck spin Hamiltonian ($-J_{12}\cdot\boldsymbol{S}_1\cdot\boldsymbol{S}_2$) derived from the broken-symmetry approach (Eq. (1)) [44]. The exchange coupling of a wide variety of compounds (see Table 2) was calculated, and this confirms that Eq. (1) is well suited for complexes with weak or strong orbital overlap [45]. Eqs. (2) and (3) describe the spin-projected and spin-unprojected Hamiltonians, respectively, and these were used for the calculations of J shown in Table 3 [44–50]. Various methods with combinations of different software packages, functionals and basis sets were used in this benchmark study [51]. As emerges from Table 1 and Fig. 5, acceptable accuracy is obtained with the Jaguar/B3LYP/6-31G*_TZVP setup, i.e., only marginally better results were obtained with combinations which lead to significantly slower convergence.

$$J_{12} = \frac{E^{BS} - E^{HS}}{\langle S\rangle_{HS}^2 - \langle S\rangle_{BS}^2} \quad (1)$$

$$J_{12} = \frac{E^{BS} - E^{HS}}{2S_1S_2} \quad (2)$$

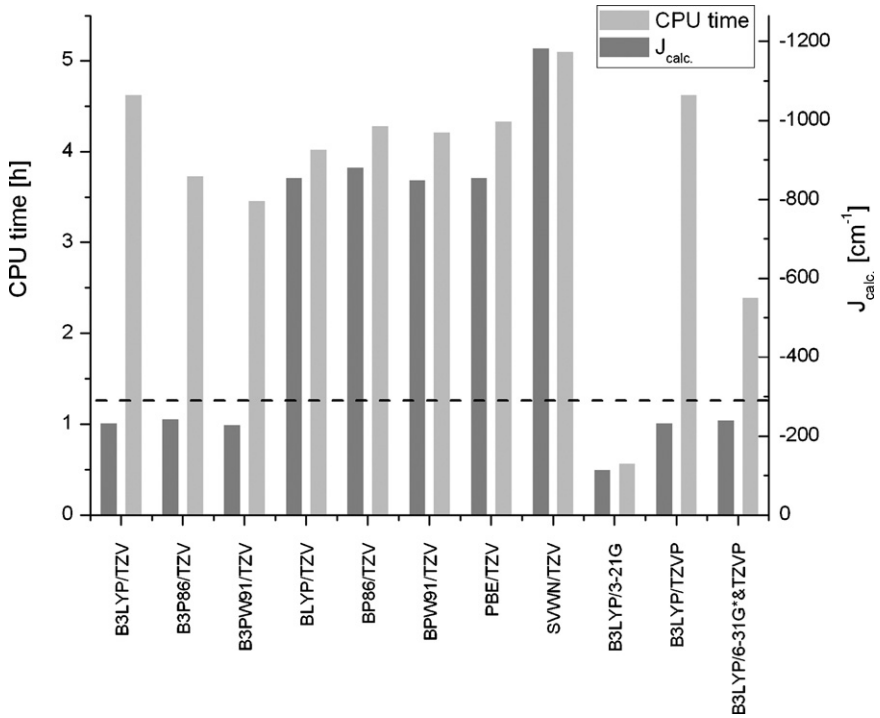

Fig. 5. CPU time required for the computation of the J value (QuadCore Q9450 (one processor), 8GB RAM; light gray) and accuracy compared with the experimental value of J (dashed line, $J = -298$ cm^{-1} [41,42]) of the bisphenolate-bridged dicopper(II) complex shown in Fig. 4, as a function of the method used (see Table 1) [43].

$$J_{12} = \frac{E^{BS} - E^{HS}}{2S_1S_2 + S_2} \quad (3)$$

An important observation is that some of the major inaccuracies are due to problems related to inaccurate or inappropriate molecular structures (see Table 2) [43]. This is not unexpected because the computational results reported in Table 1 and Fig. 5 are based on single-point calculations, and some of the experimental structural data might not be accurate enough. In addition, there might be discrepancies between the experimentally determined potential energy minima and those related to the wave functions used for the computation of the exchange coupling constants *J*. Quite generally, a preoptimized structure, based on the experimentally observed geometry, leads therefore to better agreement between the computed and observed electronic parameters (see Table 2) [43]. This is encouraging for the computational determination of the structure and electronics of novel and experimentally not yet available compounds. However, the design of novel SMM materials also requires a thorough conformational analysis and, with a full quantum-chemical structure optimization, this seems to be too demanding. Our present view – although not fully tested in all details – is that the conformational search and structure optimization steps may or need to be based on force field calculations, and it appears that these are not only much more efficient but presumably also more accurate [15]. For comparison, *J* values have also been calculated with various approaches for the Fe–CN–Cu pair, and this is shown in Table 3 [38].

4. Magnetic anisotropy

We have developed a combined ligand-field-theory/broken-symmetry-DFT approach (LFDFT) [84,85] to compute electronic parameters related to the magnetic anisotropy of oligonuclear transition metal complexes, specifically of spin clusters based on the Fe^{III}–CN–M^{II} (M = Ni, Cu) exchange coupled pair [13]. This approach takes advantage of both DFT and ligand field theory. With the complete set of Slater determinants due to all possible distributions of the *d*-electrons in the respective molecular orbitals, LFDFT derives their energies on the basis of a common set of orbitals, obtained in average-of-configuration DFT calculations. The resulting energies and the use of the composition of the 3*d* orbitals, expressed in terms of the corresponding standard basis functions (d_{xy}, d_{yz}, d_{z2}, d_{xz}, $d_{x2\text{-}y2}$) yields the interelectronic repulsion Racah parameters *B* and *C* and the (5 × 5) matrix of the ligand field. In contrast to a parameterization as used in the angular overlap model, this produces all parameters without additional approximations such as parameter additivity and transferability and allows one to treat low-symmetry complexes without the difficulty of over-parameterization. In the case of oligonuclear complexes, this procedure is repeated for each mononuclear subunit and, for ions with ground states $S > 1/2$, yields multiplet energies and values for the **g**- and zero-field splitting tensors for each subunit.

Table 3
The exchange coupling energy (*J*, in cm^{-1}, $H_{exc} = -JS_1S_2$) for the exchange pair Fe^{III}–CN–$Cu^{II}(d_{z2})$ from DFT broken spin DFT calculations with (SP) and without (SUP) spin-projection (Eqs. (2) and (3), respectively), in dependence of the adopted functional and electronic configuration of Fe^{III}, and in comparison with experimental data [38], computed with ADF [140].

Functional	$b_2^1e^4$ J_{SP}[a](J_{SUP})[b]	$b_2^2e^3$ J_{SP}[a](J_{SUP})[b]
VWN	−45.2(−22.6)	114.6(57.3)
PW91	−67.7(−33.9)	95.2(47.6)
PBE	−69.2(−34.7)	95.2(47.6)
OPBE	−112.9(−56.5)	103.2(51.6)
B3LYP 20% HF	−6.4(−3.2)	27.4(13.7)
B1LYP 25%	1.6(0.8)	19.4(9.7)
B3LYP* 15% HF	−16.2(−8.1)	35.5(17.7)
Exp	17[c]; 13.8; 3.9[d]	20.9[e]; 5.0[f]

[a] Calculated with the spin-projected formula Eq. (2), E_{BS} and E_{HS} are the energies of the (↑↓) broken-spin and the (↑↑) high-spin Slater determinants, respectively.

[b] Calculated with the spin-unprojected formula Eq. (3).

[c] Reported from a fit to magnetic susceptibility data of the Cu_3Fe_2 SMM with a $d_{x2\text{-}y2}$ ground state of Cu [97]; to compare with the calculated numbers (d_{z2} ground state of Cu^{II}), the experimental energy has to be multiplied by $2/\sqrt{3}$ ($Jd_{z2} = 2/\sqrt{3}Jd_{x2\text{-}y2}$).

[d] Reported for the two distinct Fe^{III}–CN–Cu^{II} exchange coupled pairs in the $Fe^{III}{}_2Cu^{II}{}_3$ complex [{Cu(rac-CTH)}$_3${Fe(CN)$_6$}$_2$]·2H_2O, rac-CTH = rac-5,7,7,12,14,14-hexamethyl-1,4,8,11-tetraazacyclotetradecane from simulations using a Heisenberg Hamiltonian [141].

[e] Reported from Monte Carlo simulations of the magnetic properties of heterobimetallic chain {[Fe^{III}(bpym)$(CN)_4$]$_2$ M^{II} $(H_2O)_2$}·6H_2O, bpym = 2,2′-bipyrimidine using an isotropic Heisenberg model [142].

[f] Reported from a fit of the isotropic *J* to magnetic susceptibility data on the bimetallic complex [{Fe^{III}(phen)$(CN)_4$}$_2$$Cu^{II}(H_2O)_2$]·4$H_2O$ [143].

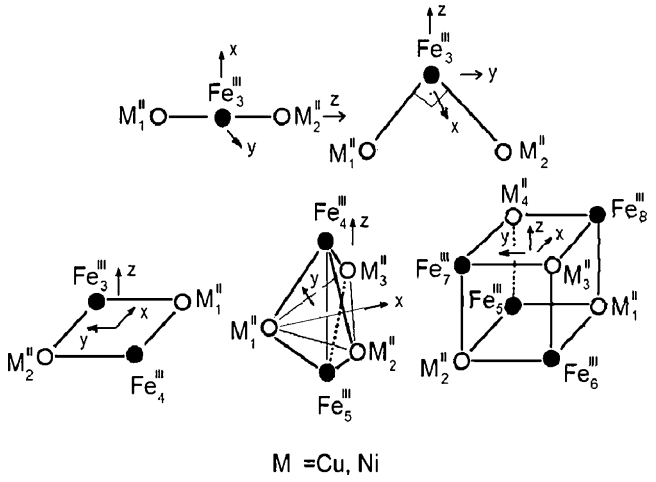

Fig. 6. Visualization of the vector coupling model and the corresponding spin Hamiltonian for the computation of the electronic parameters of oligonuclear complexes derived from dinuclear building blocks (reproduced from [13]).

For the magnetic exchange, the oligonuclear complex is subdivided into pairs to consider magnetic coupling separately within each pair. Three-center interactions, which yield much smaller contributions, are neglected [86]. With the focus on a given pair (e.g. Fe^{III}–CN–Cu^{II}), the exchange operator is introduced in a general form which, for singly occupied orbitals on Fe^{III} and Cu^{II} interchanges spins and orbitals independently and preserves invariance with respect to unitary transformations from one coordinate system to the other. For example, for the $^2T_{2g}$ ground state of $[Fe(CN)_6]^{3-}$ [87], the exchange operator operates only on the orbitals and spins of the singly occupied d_{yz}, d_{xz} and d_{xy} orbitals within the $t_{2g}{}^5$ configuration of Fe^{III} but considers the effect of all other orbital configurations in a perturbative way. This is justified by the rather large value of 10 Dq for CN^- and yields large energy separations between the $^2T_{2g}$ ground state and the excited states. To approximate the parameters of the exchange Hamiltonian (i.e., the exchange coupling energies) a C_{4v} pseudo-symmetry for each pair with the local axis *Z* along the Fe^{III}–CN–M^{II} bridge (M = Cu, Ni) was assumed to define the two exchange parameters $J_{yz,yz} = J_{xz,xz} = J_E$ and $J_{xyxy} = J_{B2}$ for the Fe^{III}–CN–M^{II} pair (off-diagonal terms vanish in this symmetry). This allows one to use DFT and the broken-symmetry approach to calculate the parameters J_E and J_{B2} from first principles. Jahn–Teller splitting of $[Fe(CN)_6]^{3-}$ is small but usually exceeds the energies of J_E and J_{B2}. Therefore, one can start from orbitals which diagonalize the Jahn–Teller vibronic coupling Hamiltonian, and account for the exchange in a second step. A procedure has been developed to deduce the tensors of the spin-Hamitonian related to the Fe^{III}–M^{II} pairs (M = Cu, Ni) from a comparison between the lowest spin states, deduced from the

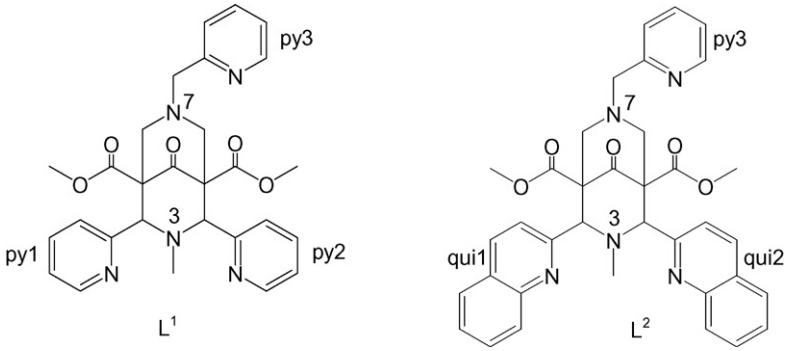

Scheme 1.

explicit calculations described above, with calculations based on the treatment of Fe^{III}–Cu^{II} or Fe^{III}–Ni^{II} pairs as a spin-only system with two $S = 1/2$ spins (M = Cu^{II}), or $S = 1/2$ and $S = 1$ spins (M = Ni^{II}), respectively [13]. The spin Hamiltonian of such a pair can be represented, taking full account of the multiplet structure due to the $[Fe(CN)_6]^{3-}$ complex [13]. A generalization of this approach to coupled pairs of any transition metal ions M^1 and M^2 and without the approximation of an axial symmetry has also been described [88].

A vector coupling scheme has been developed, which allows combining the spin Hamiltonian parameters of linear M^1–M^2 pairs to yield electronic parameters for larger spin clusters (see Fig. 6). The total Hamiltonian is given by Eq. (4), where the single and double summations run over all ions (M^1, M^2) and over all M^1–M^2 pairs; $\boldsymbol{T}_i^*$, $\boldsymbol{T}_j^*$, and $\boldsymbol{T}_{ij}^*$ are the matrices, which transform the x_l, y_l, z_l local cartesian axes of each magnetic center [$\boldsymbol{T}_i^*(M^1)$, $\boldsymbol{T}_j^*(M^2)$] and each M^1–M^2 exchange-coupled pair ($\boldsymbol{T}_{ij}^*$) into the global x, y, z axes; $\mathbf{S}_i$ and $\mathbf{S}_j$ are the spin operators in the global frame; $\mathbf{D}_{ij}$ ($\mathbf{A}_{ij}$) and $\mathbf{D}_j$ are the zero-field splitting tensors due to exchange and the single center anisotropy, respectively (the latter relate to ions such as Ni^{II} ($S = 1$) or *high-spin* Mn^{III} ($S = 2$) with local spins S larger than 1/2. The important and unique feature of this scheme in combination with the LFDFT approach is that it allows treating large magnetic spin clusters on the basis of also accounting for subtle electronic effects such as ligand field distortions and spin-orbit coupling.

$$\hat{H}_{\text{total}} = \sum_{i\in M1, j\in M2} \{(-J_{ij})\boldsymbol{S}_i'\boldsymbol{S}_j + \boldsymbol{S}_i'(\boldsymbol{T}_{ij}\boldsymbol{D}_{ij}\boldsymbol{T}_{ij}^*)\boldsymbol{S}_j + \boldsymbol{S}_i'(\boldsymbol{T}_{ij}\boldsymbol{A}_{ij}\boldsymbol{T}_{ij}^*)\boldsymbol{S}_j\} + \sum_{j\in M2}\{\boldsymbol{S}_j(\boldsymbol{T}_j\boldsymbol{D}_j\boldsymbol{T}_j^*)\boldsymbol{S}_j + \mu_B\boldsymbol{S}_j(\boldsymbol{T}_j\boldsymbol{g}_j\boldsymbol{T}_j^*)\boldsymbol{B}\} + \sum_{i\in \text{Fe}}\mu_B\boldsymbol{S}_i'(\boldsymbol{T}_i\boldsymbol{g}_i\boldsymbol{T}_i^*)\boldsymbol{B} \quad (4)$$

The LFDFT/vector coupling method has been used to compute the electronic properties of linear M–NC–Fe–CN–M trinuclear complexes (*trans*-Fe[M]$_2$; M = Cu^{II}, Ni^{II}) of D_{4h} symmetry with an octahedral $[Fe(CN)_6]^{3-}$ center. A comparison for the Cu^{II}-based system, of the calculated energy gap E_D between the ground and first excited states, derived from regular octahedral geometry of the $[Fe(CN)_6]^{3-}$ subunit ($E_D = -6.0\,cm^{-1}$) with that obtained for the observed Jahn–Teller-distorted geometry ($E_D = -0.14\,cm^{-1}$), reveals that the anisotropy energy gap E_D is reduced by more than one order of magnitude when the crystallographically determined distortion of the $[Fe(CN)_6]^{3-}$ site is taken into account [14]. Therefore, it appears that small structural changes result in relatively large modifications of the anisotropy. It follows that highly accurate structural predictions are required to fully interpret experimental data or to design novel complexes with specific magnetic properties (see also Sections 1 and 6) [15]. In addition to the linear model complexes *trans*-Fe[M]$_2$ discussed above, bent trinuclear complexes *cis*-Fe[M]$_2$ with a linear C_{4v} pseudo-symmetry of the two M–NC–Fe subunits and an M–Fe–M angle of 90° have also been studied and shown, for the Cu^{II} system, to produce a relatively small energy gap parameter ($E_D = -2.0\,cm^{-1}$). Similar to *trans*-Fe[CuL]$_2$, the parameter E_D in *cis*-Fe[CuL]$_2$ was extremely small when the observed distorted structure was used for the calculation of the term energies ($E_D = -0.11\,cm^{-1}$). However, in contrast to the linear system, the bent trinuclear complex (*cis*- vs. *trans*-Fe[CuL]$_2$) has a significant magnetic anisotropy, as shown by the calculated ground state g-tensor. That is, in contrast to *trans*-Fe[Cu]$_2$, distortions in *cis*-Fe[Cu]$_2$ increase the anisotropy. In addition to the symmetry of the Fe^{III} site, the linearity of the Fe–CN–Cu bridge also significantly affects the anisotropy. However, the values of J(Fe–Cu) are very similar for the *cis* and *trans* complexes (24.0 and 25.4 cm^{-1}, respectively), that is the non-linearity of the CN^- bridge does not affect the Cu–Fe exchange coupling in the investigated range of structures to a large extent [14].

Pentacoordinate complexes of the divalent metal ions M^2 = Mn^{II} ($S = 5/2$), Ni^{II} ($S = 1$) and Cu^{II} ($S = 1/2$) with the pentadentate bispidine ligands L^1 and L^2 (see Scheme 1) are excellent building blocks for the assembly of the hexacyanometalate-based trinuclear M^2–NC–M^1–CN–M^2 complexes discussed above [M^1 = Cr^{III} ($S = 3/2$), Fe^{III} ($S = 1/2$), Co^{III} ($S = 0$)]. In particular, these bispidine ligands selectively stabilize the linear or bent configurations, *trans*-$M^1[M^2]_2$ and *cis*-$M^1[M^2]_2$, respectively; two of the corresponding structures are shown in Fig. 7 [14]. Moreover, the architecture of the bispidine complexes allows, in particular for the Jahn–Teller active Cu^{II} complexes, to stabilize a conformation with an elongation perpendicular to the M^1–CN–M^2 axis and a concomitant short M^2–NC bond, which is predicted to yield maximum magnetic anisotropy (see above) [20,89–92].

Magnetic susceptibility and field-dependent magnetization data of these systems indicate an efficient ferromagnetic exchange coupling which leads to ferromagnetic ground states in complexes with the bispidine-based Fe^{III}–Cu^{II} and Fe^{III}–Ni^{II} exchange-coupled pairs. The analysis of the magnetic data of *trans*-Fe[Cu]$_2$ and *cis*-Fe[Cu]$_2$ with the extended Heisenberg model described above leads to the conclusion that the absence of SMM behavior in these examples is, as expected, due to the large angular distortions of the $[Fe(CN)_6]^{3-}$ central unit and the concomitant quenching of orbital angular momentum of the Fe^{III} ($^2T_{2g}$) ground state. However, it is also clear from the model calculations that small distortions due to packing forces and ligand-induced strain may reduce the magnetic and increase the transverse anisotropy due to the non-axial geometry of the bispidine $M^{II}L^1$ and $M^{II}L^2$ building blocks, and this contributes to a fast relaxation of the magnetization and therefore leads to a loss of the expected SMM behavior. Based on these and other calculations, qualitative rules for a rational design of $[Fe(CN)_6]^{3-}$ based SMMs have been formulated [13,14]:

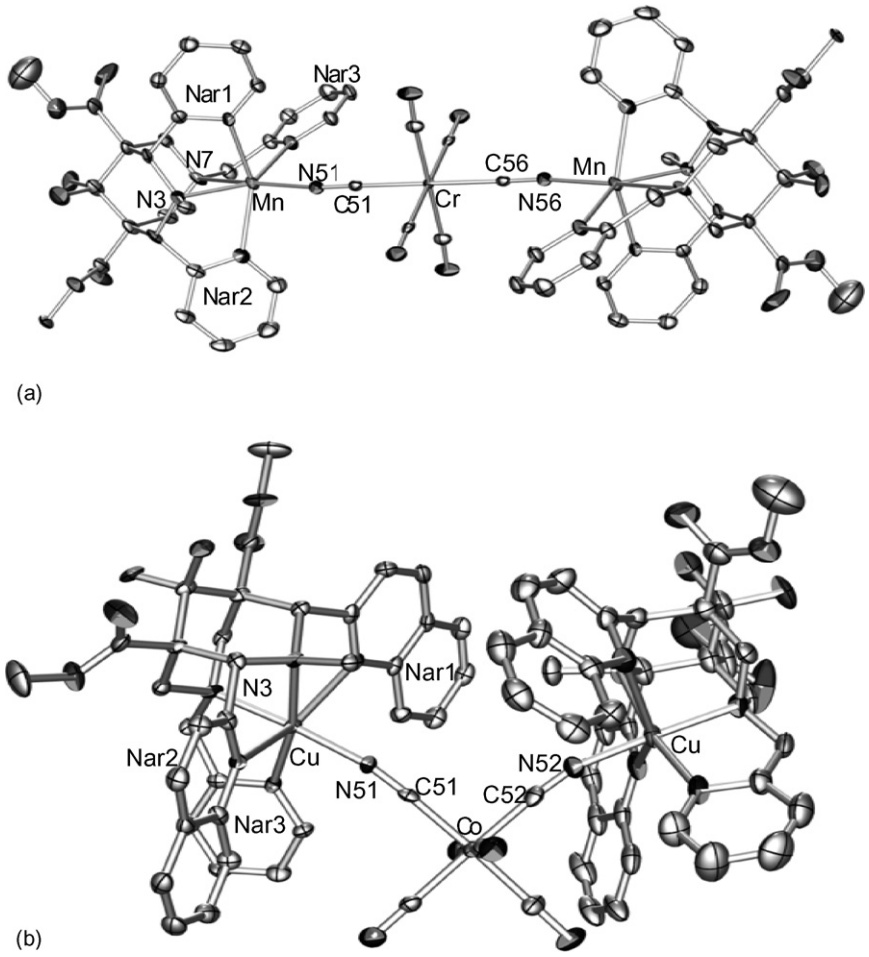

Fig. 7. Plots of the experimental structures of (a) *trans*-Cr[MnL^1]$_2$ and (b) *cis*-Co[CuL^2] [14].

1. A large magnetic anisotropy with an easy axis of magnetization along the cyanide bridge is predicted for Fe^{III}–M^{II} (M = Ni, Cu) pairs with linear Fe^{III}–CN–M^{II} geometry and regular $[Fe(CN)_6]^{3-}$ octahedra. An enhancement of the exchange anisotropy is predicted when combined with the single ion anisotropy of Ni^{II} with a negative sign of D ($M_s = \pm 1 < M_s = 0$ splitting of the $S = 1$ ground state of Ni^{II}). This implies tetragonally compressed $Ni^{II}L_6$ octahedra with a tetragonal axis aligned along the bridge.
2. In contrast to the Mn^{III}-based SMMs [9,93–95], Jahn–Teller coupling is not generally in favor of SMM behavior in spin clusters composed of Fe^{III}–Cu^{II} and Fe^{III}–Ni^{II} cyanide-bridged exchange-coupled pairs. Both Cu^{II} and Fe^{III} are Jahn–Teller active; for Fe^{III} the Jahn–Teller coupling is relatively small but of the same order of magnitude as the spin-orbit coupling interaction. A trigonal distortion of the $[Fe(CN)_6]^{3-}$ site of as little as 2° to 3° is able to reduce the spin anisotropy gap energy ($-E_D$ or U) in the Fe^{III}–Cu^{II} and Fe^{III}–Ni^{II} pairs and also in the trinuclear *trans*-Cu–Fe–Cu and *trans*-Ni–Fe–Ni complexes. Therefore, in the design of SMM materials, the influence of the angular geometry of the Fe^{III} site on the electronic structure is of great importance. Due to the strength of the Fe–CN bond, distortions of the Fe–CN fragment are less important, except for mixed ligand Fe^{III} sites (e.g., in $[Fe(Tp)(CN)_3]^-$; Tp^- = hydrotris(pyrazolyl)borate, with an enforce trigonal geometry [96,97], and in {Fe^{III}(porphyrine)(CN)-CuN_4}-type complexes [98], with an enforced tetragonal symmetry]. Based on the t_{2g} orbital splitting, which may be as large as 2900 cm^{-1} [98], ancillary ligands may significantly modify the magnetic anisotropy. In particular, for cyanide complexes of Fe^{III} with a ligand-induced ^2E_g ground state, an increase of the magnetic anisotropy of the Fe^{III}–CN–M^{II} pairs is expected.
3. Symmetry reduction increases the magnetic anisotropy in highly symmetrical spin clusters such as M_3Fe_2 and M_4Fe_4, where partial cancellation of the Fe^{III}–Cu^{II} and Fe^{III}–Ni^{II} local anisotropy tensors occurs.
4. With Ni^{II} instead of Cu^{II} subunits in Fe^{III}–CN–M^{II} pairs the M^{II} polyhedral are more symmetrical. Also, in specific cases, the Ni^{II} fragments may add a negative single ion anisotropy contribution. This is for example the case, with a ligand-enforced tetragonal compression of the Ni^{II} site.

It follows that a careful design of and a systematic search for SMMs based on cyanometalates requires an accurate prediction and interpretation of the molecular and crystal structures. Based on earlier developments and our own recent results [14,15,92,99,100], it appears that steric constraints imposed by rigid ligands may be able to enforce orbital degeneracy and therefore to systematically increase the magnetic anisotropy in oligonuclear spin clusters.

5. Syntheses and structures

In comparison with oxo-bridged compounds, cyanide-bridged oligonuclear complexes have the considerable advantage to exclusively form linear M–CN–M′ subunits. This is a significant advantage in the design and synthesis of oligonuclear complexes with predictable structures [101–104]. Moreover, in cyanide-bridged spin

clusters with low-spin Fe^{III} and Mn^{III}, the anisotropy term $\boldsymbol{S}_1 \cdot D \cdot \boldsymbol{S}_2$ dominates over the Heisenberg exchange energy $-J \cdot \boldsymbol{S}_1 \cdot \boldsymbol{S}_2$ ($|\boldsymbol{D}| > J$) [38], and the expected relatively large negative D-values allow us to use moderate-sized oligonuclear complexes, even for respectably large values of U_{eff}. Indeed, some moderate-sized cyanide-bridged SMM materials with various structural motives have been prepared, studied and reported [97,105–108]. While many of these compounds have interesting single-chain- or single-molecule-magnetic properties, it is clear that it still is difficult to top the performance of Mn_{12}.

Preparative and structural features of oligonuclear cyanometalates have been reviewed extensively [101–104], and our own experimental studies, which are related to the theoretical work described above, have been published [14,109–111]. The most appropriate examples, i.e. those which have SMM properties [97,101,105] and those which have been used to validate our model calculations [13,14] have been discussed above.

6. Conclusions

We have shown that there are appropriate theoretical methods for predicting the exchange coupling [38,40,43] and magnetic anisotropy of paramagnetic oligonuclear transition metal complexes [13,14]. Based on these calculations it has been possible to derive qualitative rules for the design of hexacyanometalate-based SMMs [13,14]. An important and not unexpected observation is that subtle structural changes lead to significant modifications of the magnetic exchange and anisotropy and therefore generally to a lower than anticipated anisotropy barrier. Interestingly, a reduction of the anisotropy is not only observed for deviations from linearity of the M–CN–M′ bridges but, more importantly, for deviations from tetragonal symmetry of the hexacyanometalate sites, and these often are the result of Jahn–Teller coupling. It emerges that the ligand-enforced control of the coordination geometry is an important tool for the design of novel SMM materials [15,99,112]. Also, the design must be based on efficient and accurate methods for the structural modeling which then may be followed by single-point calculations of the electronic parameters. We have shown here that, based on LFDFT, broken symmetry DFT and a vector coupling approach, there are efficient methods for the prediction of the electronic properties. It is our belief that molecular mechanics calculations are not only much more efficient but, with the correct method and force field, also lead to very accurate optimized geometries [20,100,113–120]. Therefore, apart from the need for viable preparative methods, the major requirement for developing novel and efficient SMMs seems to be in the area of efficient and accurate structure optimization.

Acknowledgements

Our own contributions are generously supported by the University of Heidelberg and the German Science Foundation (DFG, SPP1137 “Molecular Magnetism”). We are grateful for this invaluable help and the many scientific contributions of our coworkers and collaboration partners, whose names appear in the references.

References

[1] T. Lis, Acta Crystallogr. B 36 (1980) 2042.
[2] A. Caneschi, D. Gatteschi, R. Sessoli, A.L. Barra, L.C. Brunel, M. Guillot, J. Am. Chem. Soc. 113 (1991) 5873.
[3] R. Sessoli, H.-L. Tsai, A.R. Schake, S. Wang, J.B. Vincent, K. Folting, D. Gatteschi, G. Christou, D.N. Hendrickson, J. Am. Chem. Soc. 115 (1993) 1804.
[4] R. Sessoli, D. Gatteschi, A. Caneschi, M.A. Novak, Nature 365 (1993) 141.
[5] L. Thomas, F. Lionti, R. Ballou, D. Gatteschi, R. Sessoli, B. Barbara, Nature 383 (1996) 145.
[6] H.-L. Tsai, D.-M. Chen, C.-I. Yang, T.-Y. Jwo, C.-S. Wur, G.-H. Lee, Y. Wang, Inorg. Chem. Commun. 4 (2001) 511.
[7] D. Gatteschi, A. Caneschi, R. Sessoli, in: E. Coronado, P. Delhaés, D. Gatteschi, J.S. Miller, N.A.S.E.A. Sciences (Eds.), Molecular Magnetism: From Molecular Assemblies to the Devices, Kluwer Academic Publishers, Dordrecht, 1996, p. 289.
[8] G. Aromi, S.M.J. Aubin, M.A. Bolcar, G. Christou, H.J. Eppley, K. Folting, D.N. Hendrickson, J.C. Huffman, R.C. Squire, H.-L. Tsai, S. Wang, M.W. Wemple, Polyhedron 17 (1998) 3005.
[9] R. Sessoli, D. Gatteschi, Angew. Chem. Int. Ed. 42 (2003) 268.
[10] J.R. Long, in: P. Yang (Ed.), Molecular Cluster Magnets in Chemistry of Nanostructured Materials, World Scientific, Hong Kong, 2003, p. 291.
[11] C.J. Milios, A. Vinslava, W. Wernsdorfer, S. Moggach, S. Parsons, S.P. Perlepes, G. Christou, E.K. Brechin, J. Am. Chem. Soc. 129 (2007) 2754.
[12] O. Kahn, Molecular Magnetism, Wiley & Sons Inc., New York, 1993.
[13] M. Atanasov, P. Comba, C.A. Daul, Inorg. Chem. 47 (2008) 2449.
[14] M. Atanasov, C. Busche, P. Comba, F. El Hallak, B. Martin, G. Rajaraman, J. van Slageren, H. Wadepohl, Inorg. Chem. 47 (2008) 8112.
[15] P. Comba, M. Kerscher, Coord. Chem. Rev. 253 (2009) 564.
[16] C. Diedrich, R.J. Deeth, Inorg. Chem. 47 (2008) 2494.
[17] R.J. Deeth, N. Fey, B.J. Williams-Hubbard, J. Comp. Chem. 26 (2005) 123.
[18] R.J. Deeth, L.J.A. Hearnshaw, J. Chem. Soc., Dalton Trans. (2006) 1092.
[19] R.J. Deeth, Inorg. Chem. 46 (2007) 4492.
[20] A. Bentz, P. Comba, R.J. Deeth, M. Kerscher, H. Pritzkow, B. Seibold, H. Wadepohl, Inorg. Chem. 47 (2008) 9518.
[21] J. Sabolovic, Polyhedron 12 (1993) 1107.
[22] B. Kaitner, N. Paulic, G. Pavlovic, J. Sabolovic, Polyhedron 18 (1999) 2301.
[23] J. Sabolovic, K.R. Liedl, Inorg. Chem. 38 (1999) 2764.
[24] M.U. Schmidt, in: D. Braga, F. Grepioni, A.G. Orpen (Eds.), Crystal Engineering From Molecules and Crystals to Materials, Kluwer Academic Publishers, Dordrecht, The Netherlands, 1999, p. 331.
[25] F. Schütz, P. Kopietz, V. Paschenko, B. Wolf, M. Lang, J.W. Bats, C. Hu, U.M. Schmidt, Phys. Rev. B72 (2005) 174429.
[26] S. Reichling, G. Huttner, Eur. J. Inorg. Chem. (2000) 857.
[27] H. Weihe, H.U. Güdel, Comments Inorg. Chem. 22 (2000) 75.
[28] V.S. Mironov, L.F. Chibotaru, A. Ceulemans, J. Am. Chem. Soc. 125 (2003) 9750.
[29] M. Verdaguer, A. Bleuzen, C. Train, G.R.F.F. deBiani, Philos. Trans. R. Soc. London Ser. A 357 (1999) 2959.
[30] M. Verdaguer, A. Bleuzen, V. Marvaud, J. Vaissermann, M. Seuleiman, C. Desplanches, A. Scuiller, C. Train, G.R.G. Gelly, C. Lomenech, I. Rosenman, P. Veillet, C. Cartier, F. Villain, Coord. Chem. Rev. 192 (1999) 1023.
[31] O. Kahn, B. Briat, J. Chem. Soc., Faraday Trans. 1 72 (1976) 268.
[32] O. Kahn, B. Briat, J. Chem. Soc., Faraday Trans. 1 72 (1976) 1441.
[33] V. Eyert, B. Siberchicot, M. Verdaguer, Phys. Rev. B 56 (1997) 8959.
[34] N.M. Harrison, B.G. Searle, E.A. Seddon, Chem. Phys. Lett. 266 (1997) 507.
[35] M. Nishino, S. Takeda, W. Mori, A. Nakamura, K. Yamaguchi, Synth. Met. 85 (1997) 1763.
[36] M. Nishino, Y. Yoshioka, K. Yamaguchi, Chem. Phys. Lett. 297 (1998) 51.
[37] E. Ruiz, A. Rodriguez-Fortea, S. Alvarez, M. Verdaguer, Chem. Eur. J. 11 (2005) 2135.
[38] M. Atanasov, P. Comba, C.A. Daul, J. Phys. Chem. A 110 (2006) 13332.
[39] I.B. Bersuker, J. Comput. Chem. 18 (1997) 260.
[40] M. Atanasov, P. Comba, C.A. Daul, A. Hauser, J. Phys. Chem. (A) 111 (2007) 9145.
[41] G.A. Barclay, C.M. Harris, B.F. Hoskins, E. Kokot, Proc. Chem. Soc. (1961) 264.
[42] B. Jczowska-Trzebiatowska, J. Jczierska, J. Baranowski, Chem. Phys. Lett. 52 (1977) 590.
[43] P. Comba, S. Hausberg, B. Martin, submitted for publication.
[44] L. Noodleman, J. Chem. Phys. 74 (1981) 5737.
[45] T. Soda, Y. Kitagawa, T. Onishi, Y. Takano, Y. Shigeta, H. Nagao, Y. Yoshioka, K. Yamaguchi, Chem. Phys. Lett. 319 (2000) 223.
[46] L. Noodleman, E.R. Davidson, Chem. Phys. 109 (1986) 131.
[47] K. Yamaguchi, T. Yakahara, T. Fueno, in: V.H. Smith (Ed.), Applied Quantum Chemistry, V. Reidel, Dordrecht, 1986, p. 155.
[48] E. Ruiz, J. Cano, S. Alvarez, P. Alemany, J. Comput. Chem. 20 (1999) 1391.
[49] E. Ruiz, A. Rodriguez-Fortea, J. Cano, S. Alvarez, P. Alemany, J. Comp. Chem. (2003) 982.
[50] E. Ruiz, S. Alvarez, J. Cano, J. Chem. Phys. 123 (2005) 164110.
[51] Gaussian [52], Jaguar [53], ORCA [54]; functionals: B3LYP [55–57], B3P86 [58], B3PW91 [59], BLYP [60–62], BP86 [58,60–62], BPW91 [59–62], PBE [63], SVWN [64,65]; basis sets: 3-21G [66–71], TZV [72,73], TZVP [72,73], 6-31G* [74–83].
[52] M.J. Frisch, G.W. Trucks, H.B. Schlegel, G.E. Scuseria, M.A. Robb, J.R. Cheeseman, J.A. Montgomery Jr., T. Vreven, K.N. Kudin, J.C. Burant, J.M. Millam, S.S. Iyengar, J. Tomasi, V. Barone, B. Mennucci, M. Cossi, G. Scalmani, N. Rega, G.A. Petersson, H. Nakatsuji, M. Hada, M. Ehara, K. Toyota, R. Fukuda, J. Hasegawa, M. Ishida, T. Nakajima, Y. Honda, O. Kitao, H. Nakai, M. Klene, X. Li, J.E. Knox, H.P. Hratchian, J.B. Cross, V. Bakken, C. Adamo, J. Jaramillo, R. Gomperts, R.E. Stratmann, O. Yazyev, A. Austin, R. Cammi, C. Pomelli, J.W. Ochterski, P.Y. Ayala, K. Morokuma, G.A. Voth, P. Salvador, J.J. Dannenberg, V.G. Zakrzewski, S. Dapprich, A.D. Daniels, M.C. Strain, O. Farkas, D.K. Malick, A.D. Rabuck, K. Raghavachari, J.B. Foresman, J.V. Ortiz, Q. Cui, A.G. Baboul, S. Clifford, J. Cioslowski, B.B. Stefanov, G. Liu, A. Liashenko, P. Piskorz, I. Komaromi, R.L. Martin, D.J. Fox, T. Keith, M.A. Al-Laham, C.Y. Peng, A. Nanayakkara, M. Challacombe, P.M.W. Gill, B. Johnson, W. Chen, M.W. Wong, C. Gonzalez, J.A. Pople, Gaussian 03, Revision B.03, Gaussian Inc., Wallingford CT, 2003.
[53] Schrödinger, JAGUAR 5.5. Schrödinger LLC, New York, NY, 2005.

[54] F. Neese, ORCA, version 2.4, an ab initio, density functional and semiempirical program package, Max-Planck-Institut für Bioanorganische Chemie: Mülheim an der Ruhr, Germany, 2005.
[55] A.D. Becke, J. Chem. Phys. 96 (1992) 2155.
[56] A.D. Becke, J. Chem. Phys. 97 (1992) 9713.
[57] A.D. Becke, J. Chem. Phys. B 98 (1993) 5648.
[58] J.P. Perdew, Phys. Rev. B 33 (1986) 8822.
[59] J.P. Perdew, K. Burke, Y. Wang, Phys. Rev. B 54 (1996) 16533.
[60] A.D. Becke, Phys. Rev. A 38 (1988) 3098.
[61] C. Lee, W. Yang, R.G. Parr, Phys. Rev. B 37 (1988) 785.
[62] B. Miehlich, A. Savin, H. Stoll, H. Preuss, Chem. Phys. Lett. 157 (1989) 200.
[63] J.P. Perdew, K. Burke, M. Ernzerhof, Phys. Rev. Lett. 77 (1996) 3865.
[64] P. Hohenberg, W. Kohn, Phys. Rev. 136 (1964) B864.
[65] S.H. Vosko, L. Wilk, M. Nusair, Can. J. Phys. 58 (1980) 1200.
[66] J.S. Binkley, J.A. Pople, W.J. Hehre, J. Am. Chem. Soc. 102 (1980) 939.
[67] M.S. Gordon, J.S. Binkley, J.A. Pople, W.J. Pietro, W.J. Hehre, J. Am. Chem. Soc. 104 (1982) 2797.
[68] W.J. Pietro, M.M. Francl, W.J. Hehre, D.J. Defrees, J.A. Pople, J.S. Binkley, J. Am. Chem. Soc. 104 (1982) 5039.
[69] K.D. Dobbs, W.J. Hehre, J. Comp. Chem. 7 (1986) 359.
[70] K.D. Dobbs, W.J. Hehre, J. Comp. Chem. 8 (1987) 861.
[71] K.D. Dobbs, W.J. Hehre, J. Comp. Chem. 8 (1987) 880.
[72] A. Schäfer, H. Horn, R. Ahlrichs, J. Chem. Phys. 97 (1992) 2571.
[73] A. Schäfer, C. Huber, R. Ahlrichs, J. Chem. Phys. 100 (1994) 5829.
[74] R. Ditchfield, W.J. Hehre, J.A. Pople, J. Chem. Phys. 54 (1971) 724.
[75] W.J. Hehre, R. Ditchfield, J.A. Pople, J. Chem. Phys. 56 (1972) 2257.
[76] P.C. Hariharan, J.A. Pople, Mol. Phys. 27 (1974) 209.
[77] M.S. Gordon, Chem. Phys. Lett. 76 (1980) 163.
[78] P.C. Hariharan, J.A. Pople, J. Chem. Phys. 82 (1973) 213.
[79] J.-P. Blaudeau, M.P. McGrath, L.A. Curtiss, L. Radom, J. Chem. Phys. 107 (1997) 5016.
[80] M.M. Francl, W.J. Pietro, W.J. Hehre, J.S. Binkley, D.J. DeFrees, J.A. Pople, M.S. Gordon, J. Chem. Phys. 77 (1982) 3654.
[81] R.C. Binning Jr., L.A. Curtiss, J. Comp. Chem. 11 (1990) 1206.
[82] V.A. Rassolov, J.A. Pople, M.A. Ratner, T.L. Windus, J. Chem. Phys. 109 (1998) 1223.
[83] V.A. Rassolov, M.A. Ratner, J.A. Pople, P.C. Redfern, L.A. Curtiss, J. Comp. Chem. 22 (2001) 976.
[84] M. Atanasov, C.A. Daul, C. Rauzy, Chem. Phys. Lett. 367 (2003) 737.
[85] M. Atanasov, C.A. Daul, C. Rauzy, Struct. Bond. 106 (2004) 97.
[86] K.I. Gondaira, Y. Tanabe, J. Phys. Soc. Jpn. 21 (1966) 1527.
[87] Orbital effects of Cu^{II} into given effective values of its g-tensor are included.
[88] M. Atanasov, P. Comba, The Jahn-Teller Effect. Advances and Perspectives, in: H. Köppel, H. Barentzen, D.R. Yarkony (Eds.), Springer Series of Chemical Physics. Springer, Heidelberg, 2009, accepted.
[89] P. Comba, M. Kerscher, M. Merz, V. Müller, H. Pritzkow, R. Remenyi, W. Schiek, Y. Xiong, Chem. Eur. J. 8 (2002) 5750.
[90] P. Comba, A. Hauser, M. Kerscher, H. Pritzkow, Angew. Chem. Int. Ed. 42 (2003) 4536.
[91] P. Comba, C. Lopez de Laorden, H. Pritzkow, Helv. Chim. Acta 88 (2005) 647.
[92] P. Comba, M. Kerscher, W. Schiek, Prog. Inorg. Chem. 55 (2008) 613.
[93] D. Gatteschi, R. Sessoli, J. Villain, Molecular Nanomagnets, Oxford University Press, Oxford, 2006.
[94] M.F. Anderlund, J. Zheng, M. Ghiladi, M. Kritikos, E. Rivière, L. Sun, J.-J. Girerd, B. Akermark, Inorg. Chem. Commun. 9 (2006) 1195.
[95] H. Oshio, M. Nakano, Chem. Eur. J. 11 (2005) 5178.
[96] B.M. Bartlett, T. David Harris, M.W. DeGroot, J.R. Long, Z. Anorg. Allg. Chem. 633 (2007) 2380.
[97] C.-F. Wang, J.-L. Zuo, B.M. Bartlett, Y. Song, J.R. Long, X.-Z. You, J. Am. Chem. Soc. 128 (2006) 7162.
[98] M.J. Gunter, K.J. Berry, K.S. Murray, J. Am. Chem. Soc. 106 (1984) 4227.
[99] P. Comba, W. Schiek, Coord. Chem. Rev 238–239 (2003) 21.
[100] A. Bentz, P. Comba, R.J. Deeth, M. Kerscher, B. Seibold, H. Wadepohl, Inorg. Chem. 47 (2008) 9518.
[101] L.M.C. Beltran, J.R. Long, Acc. Chem. Res. 38 (2005) 325.
[102] T. Mallah, C. Auberger, M. Verdaguer, P. Veillet, J. Chem. Soc., Chem. Commun. (1995) 61.
[103] C.P. Berlinguette, D.H. Vaughan, C. Canada-Vilalta, J.R. Galán Mascarós, K.R. Dunbar, Angew. Chem. Int. Ed. 42 (2003) 1523.
[104] J.-N. Rebilly, T. Mallah, Struct. Bond. 122 (2006) 103.
[105] H.J. Choi, J.J. Sokol, J.R. Long, Inorg. Chem. 43 (2004) 1606.
[106] S.I. Klokishner, S.M. Ostrovsky, A.V. Palii, K.R. Dunbar, J. Mol. Struct. 838 (2007) 144.
[107] E.J. Schelter, F. Karadas, C. Avendano, A.V. Prosvirin, W. Wernsdorfer, K.R. Dunbar, J. Am. Chem. Soc. 129 (2007) 8139.
[108] M. Ferbinteanu, H. Miyasaka, W. Wernsdorfer, K. Nakata, K. Sugiura, M. Yamashita, C. Coulon, R. Clérac, J. Am. Chem. Soc. 127 (2005) 3090.
[109] M. Atanasov, P. Comba, Y.D. Lampeka, G. Linti, T. Malcherek, R. Miletich, A.I. Prikhod'ko, H. Pritzkow, Chem. Eur. J. 12 (2006) 737.
[110] M. Atanasov, P. Comba, S. Förster, G. Linti, T. Malcherek, R. Miletich, A. Prikhod'ko, H. Wadepohl, Inorg. Chem. 45 (2006) 7722.
[111] P. Comba, G. Hanson, S. Helmle, H. Wadepohl, publication in preparation.
[112] C. Buning, G.W. Canters, P. Comba, C. Dennison, L. Jeuken, M. Melter, J. Sanders-Loehr, J. Am. Chem. Soc. 122 (2000) 204.
[113] P. Comba, M. Zimmer, Inorg. Chem. 33 (1994) 5368.
[114] J.E. Bol, C. Buning, P. Comba, J. Reedijk, M. Ströhle, J. Comput. Chem. 19 (1998) 512.
[115] P. Comba, Coord. Chem. Rev. 182 (1999) 343.
[116] P. Comba, Coord. Chem. Rev. 185 (1999) 81.
[117] P. Comba, N. Okon, R. Remenyi, J. Comput. Chem. 20 (1999) 781.
[118] J. Bartol, P. Comba, M. Melter, M. Zimmer, J. Comput. Chem. 20 (1999) 1549.
[119] P. Comba, R. Remenyi, J. Comput. Chem. 23 (2002) 697.
[120] P. Comba, R. Remenyi, Coord. Chem. Rev. 238–239 (2003) 9.
[121] H.H. Song, L.M. Zheng, Y.J. Liu, X.Q. Xin, A.J. Jacobson, S. Decurtins, J. Chem. Soc., Dalton Trans. (2001) 3274.
[122] I. Rudra, Q. Wu, T.V. Voorhis, J. Chem. Phys. 124 (2006) 024103.
[123] T.R. Felthouse, E.D. Laskowski, D.N. Hendrickson, Inorg. Chem. 16 (1977) 1077.
[124] C. Mathoniere, O. Kahn, J.C. Daran, H. Hilbig, F.H. Kohler, Inorg. Chem. 32 (1993) 4057.
[125] Y. Sun, M. Melchior, D.A. Summers, R.C. Thompson, S.J. Rettig, C. Orvig, Inorg. Chem. 37 (1998) 3119.
[126] G. Haselhorst, K. Wieghardt, S. Keller, B. Schrader, Inorg. Chem. 32 (1993) 520.
[127] S. Sinnecker, F. Neese, L. Noodleman, W. Lubitz, J. Am. Chem. Soc. 126 (2004) 2613.
[128] M. Julve, F. Lloret, F. Faus, M. Verdaguer, A. Caneschi, Inorg. Chem. 34 (1995) 157.
[129] F. Birkelbach, M. Winter, U. Florke, H.J. Haupt, C. Butzlaff, M. Lengen, E. Bill, A.X. Trautwein, K. Wieghardt, P. Chaudhuri, Inorg. Chem. 33 (1994) 3990.
[130] K. Wieghardt, U. Bossek, K. Volckmar, W. Swiridoff, J. Weiss, Inorg. Chem. 23 (1984) 1387.
[131] A. Rodríguez-Fortea, P. Alemany, S. Alvarez, E. Ruiz, Eur. J. Inorg. Chem. (2004) 143.
[132] A.S. Ceccato, A. Neves, M.A.d. Brito, S.M. Drechsel, A.S. Mangrich, R. Werner, W. Haase, A. Bortoluzzi, J. Chem. Soc., Dalton Trans. (2000) 1567.
[133] N.S. Dean, M.R. Bond, C.J. O'Connor, C.J. Carrano, Inorg. Chem. 35 (1996) 7643.
[134] S. Burojevic, I. Shweky, A. Bino, D.A. Summers, R.C. Thompson, Inorg. Chim. Acta 251 (1996) 75.
[135] A. Neves, K. Wieghardt, B. Nuber, J. Weiss, Inorg. Chim. Acta 150 (1988) 183.
[136] R. Das, K.K. Nanda, A.K. Mukherjee, M. Helliwell, K. Nag, J. Chem. Soc., Dalton Trans. (1993) 2241.
[137] M.I. Khan, Y.-D. Chang, Q. Chen, J. Salta, Y.-S. Lee, C.J. O'Connor, J. Zubieta, Inorg. Chem. 33 (1994) 6340.
[138] W. Plass, Angew. Chem. Int. Ed. Engl. 35 (1996) 627.
[139] A. Rodríguez-Fortea, P. Alemany, S. Alvarez, E. Ruiz, A. Scuiller, C. Decroix, V. Marvaud, J. Vaissermann, M. Verdaguer, I. Rosenman, M. Julve, Inorg. Chem. 40 (2001) 5868.
[140] A. Bérces, C. Bo, P.M. Boerrigter, L. Cavallo, D.P. Chong, L. Deng, R.M. Dickson, D.E. Ellis, L. Fan, T.H. Fischer, C. Fonseca Guerra, S.J.A. Van Gisbergen, J.A. Groeneveld, O.V. Gritsenko, M. Grüning, F.E. Harris, P. Van den Hoek, H. Jacobsen, G. Van Kessel, F. Kootstra, E. Van Lenthe, D.A. McCormack, V.P. Osinga, S. Patchkovskii, P.H.T. Philipsen, D. Post, C.C. Pye, W. Ravenek, P. Ros, P.R.T. Schipper, G. Schreckenbach, J.G. Snijders, M. Sola, M. Swart, D. Swerhone, G. Te Velde, P. Vernooijs, L. Versluis, O. Visser, E. Van Wezenbeek, G. Wiesenekker, S.K. Wolff, T.K. Woo, E.J. Baerends, J. Autschbach, T. Ziegler, ADF2006.01 SCM, Theoretical Chemistry, Vrije Universiteit, Amsterdam, The Netherlands, 2006.
[141] A. Rodríguez-Diéguez, R. Kivekäs, R. Sillanpää, J. Cano, F. Lloret, V. McKee, H. Stoeckli-Evans, E. Colacio, Inorg. Chem. 45 (2006) 10537.
[142] L.M. Toma, R. Lescouëzec, J. Pasán, C. Ruiz-Pérez, J. Vaissermann, J. Cano, R. Carrasco, W. Wernsdorfer, F. Lloret, M. Julve, J. Am. Chem. Soc. 128 (2006) 4842.
[143] L.M. Toma, F.S. Delgado, C. Ruiz-Pérez, R. Carrasco, J. Cano, F. Lloret, M. Julve, J. Chem. Soc., Dalton Trans. (2004) 2836.